

Analyst

Accepted Manuscript



This is an *Accepted Manuscript*, which has been through the Royal Society of Chemistry peer review process and has been accepted for publication.

Accepted Manuscripts are published online shortly after acceptance, before technical editing, formatting and proof reading. Using this free service, authors can make their results available to the community, in citable form, before we publish the edited article. We will replace this *Accepted Manuscript* with the edited and formatted *Advance Article* as soon as it is available.

You can find more information about *Accepted Manuscripts* in the [Information for Authors](#).

Please note that technical editing may introduce minor changes to the text and/or graphics, which may alter content. The journal's standard [Terms & Conditions](#) and the [Ethical guidelines](#) still apply. In no event shall the Royal Society of Chemistry be held responsible for any errors or omissions in this *Accepted Manuscript* or any consequences arising from the use of any information it contains.

1
2 **Facile synthesis of novel magnetic silica nanoparticles functionalized with**
3 **layer-by-layer detonation nanodiamonds for secretome study of human**
4 **hepatoma cell**
5
6
7

8 Hong Li¹, Yi Wang¹, Lei Zhang¹, Haojie Lu¹, Zhongjun Zhou², Liming Wei^{1*}, Pengyuan Yang^{1*}
9

10 ¹Department of Chemistry & Institutes of Biomedical Sciences, Fudan University, Shanghai,
11 200032, China
12

13 ²Department of Biochemistry, University of Hong Kong, Hong Kong, China.
14
15
16

17
18 * Authors for Correspondence
19

20 Liming Wei, Pengyuan Yang

21 Address: Department of Chemistry & Institutes of Biomedical Sciences, Fudan University, 220
22 Han Dan Road, Shanghai 200433, PR China.
23

24 E-mail: weiliming@fudan.edu.cn, pyyang@fudan.edu.cn
25

26 Phone: +86 21 5423-7443
27

28 Fax: +86 21 5423-7961
29
30
31
32
33
34
35
36
37
38
39
40
41
42
43
44
45
46
47
48
49
50
51
52
53
54
55
56
57
58
59
60

Abstract

Novel magnetic silica nanoparticles functionalized with layer-by-layer detonation nanodiamonds (dNDs) were prepared by coating single submicron-size magnetite particles with silica and subsequently modified with dNDs. The resulting layer-by-layer dNDs functionalized magnetic silica microspheres ($\text{Fe}_3\text{O}_4@\text{SiO}_2@[\text{dNDs}]_n$) exhibit well-defined magnetite-core-silica-shell structure and possess high content of magnetite, which endow them with high dispersibility and excellent magnetic responsibility. Meanwhile, dNDs is known for its high affinity and biocompatibility towards peptides or proteins. Thus, a novel convenient, fast and efficient pretreatment approach of low-abundance peptides or proteins was successfully established with $\text{Fe}_3\text{O}_4@\text{SiO}_2@[\text{dNDs}]_n$ microspheres. The signal intensity of low-abundance peptides was improved by at least two to three orders of magnitude in mass spectrometry analysis. The novel microsphere also showed good tolerance to salt. Even with high concentration of salt, peptides or proteins could be isolated effectively from sample. Therefore, the convenient and efficient enrichment process of this novel layer-by-layer dNDs-functionalized microsphere make it promising candidate for isolation of protein in huge volume of culture supernatant for secretome analysis. In the application of $\text{Fe}_3\text{O}_4@\text{SiO}_2@[\text{dNDs}]_n$ in the secretome of hepatoma cell, 1473 proteins were identified and covered a broad range of *pI* and molecular weight, including 377 low molecular weight proteins.

Keywords: Detonation nanodiamond-functionalized magnetic silica microsphere, Pretreatment, Low-abundance peptides or proteins, Secretome, Mass spectrometry

1. Introduction

The secretome, an “omic” term used to describe proteins secreted from cells or tissues, has recently received much attention due to the vital roles of secreted proteins in lots of important processes such as cell growth, development, cell signaling and binding. Profiling of cancer cell line secretomes has been shown to be a promising strategy for identifying potential cancer biomarkers [1-4]. However, analysis of secreted proteins is quite challenging due to the inherent low concentrations of secreted proteins and the presence of high amounts of interfering salts and other compounds. Therefore, pretreatment and separation of proteins is almost mandatory for subsequent secretomic analysis [3-4]. Ultrafiltration, precipitation and dialysis are the most often used pretreatment methods. However, these traditional techniques suffer from their own drawbacks. Dialysis methods are time-consuming and result in substantial protein loss, which is a critical concern when dealing with small sample volumes. Depending on the molecular weight cut off (MWCO) of the membrane followed by centrifugal vacuum drying, proteins can be purified, separated, or concentrated in either fraction by ultrafiltration approach. But ultrafiltration approach is also time-consuming and costly. As for protein precipitation, some important parameters should be considered, such as temperature, pH and protein concentration in solution. Meanwhile, the precipitates in the procedure are hardly dissolvable, thus this method gives poor protein yield [5]. Furthermore, the low molecular weight (LMW) fraction of secretome, which is considered to be a valuable reservoir of biomarkers, such as hormones, cytokines, and growth factors, are also prone to lose during the conventional pretreatment approaches. Therefore, it is an urgent task to develop novel sample preparation techniques for pretreatment of low-abundance proteins or peptides from culture supernatant.

For rapid enrichment of low-abundance proteins or peptides from biological samples, proteomics using nanotechnology resources establish a novel analytical platform known as nanoproteomics [6]. The employment of nanomaterials smaller than 100 nm to enrich low-abundance proteins or peptides provides a promising way to increase the limit of detection and identified efficiency of proteins with their unique size-related physical and chemical properties. Some scientists have developed several advanced materials for the concentration of low-abundance peptides in complex samples, including, functionalized nano-CdS (for peptides) [7], CaCO₃, ZnO₂, SnO₂ or TiO₂-poly(methyl methacrylate) nanoparticles (for peptides) [8, 9], MCM-41 porous nanoparticles (for endogenous peptides) [10] and mesoporous silica particles (for peptides in plasma) [11], polymeric beads (for peptides/proteins) [12], porous glass beads (for proteins) [13], multi-walled carbon nanotubes (for proteins) [14] and so on. In the secretome analysis, Cao et al. described a versatile and effective approach for enrichment of secreted proteins based on nanozeolites LTL (Linder type-L) [15]. Nanozeolite LTL displays the absorption of protein or peptides due to its special columned morphology and negative surface charge. However, 600 µg of nanozeolites in 10 mL of conditioned media must be centrifuged at high speed for a

1
2 long time to collect it. The concentrated secretome proteins or peptides were further eluted under
3 gel electrophoresis, which could cause low molecular weight proteins (lower than 10 KDa) loss.
4 Paule et al. also showed the combination of SEAN (size exclusion/affinity nanoparticles) and
5 proteomics enables the analysis of secreted proteins with low molecular weight and low
6 abundance [16]. However, these approaches mentioned above need centrifugation to separate
7 nanoparticles from sample, making the pretreatment process very laborious, time-consuming and
8 apt to lose low-abundant peptides because of co-separation with nanoparticles during
9 centrifugation. Therefore, searching for a simple, fast and effective enrichment process for
10 secretome analysis is urgently needed.

11
12 To make up for the shortcoming mentioned above, some surface functionalized magnetic
13 particles have been widely developed for the peptide or protein extraction and enrichment owing
14 to their distinguished properties, including high magnetic sensitivity, excellent dispersibility in
15 aqueous solution and chemical stability, which guarantee a fast, efficient magnetic separation, as
16 well as good recycling [17, 18]. Previous reports have shown that magnetic beads functionalized
17 with reversed-phase (RP) group (such as C₈-functionalized magnetic microspheres) are broadly
18 used for SPE-based strategy, which are an ideal candidate for the efficient enrichment of peptides
19 from biological samples through hydrophobic–hydrophobic interaction or hydrophilic interaction
20 [19]. Other carbon-based composites, including Fullerene (C₆₀)-functionalized magnetic
21 microspheres (Fe₃O₄@nSiO₂@C₆₀) [20], carbon nanotube (CNT)-decorated magnetic
22 microspheres and graphene-encapsulated magnetic microspheres (Fe₃O₄@nSiO₂@G) have been
23 developed for the enrichment of low-concentration peptides due to the strong hydrophobic
24 interactions between the carbon skeletons and peptides [21, 22]. However, due to the huge
25 interaction between peptides or proteins with the layer of carbon material outside the above
26 materials, the recovery of peptides or proteins isn't good. Thus, these advanced material
27 microspheres have never been applied for the secretome analysis. Functionalized magnetic
28 nanoparticles have also been developed for specific enrichment of peptides/proteins with
29 post-translational modifications, such as phosphorylation and glycosylation. For example, several
30 metal ion-immobilized magnetic nanoparticles, such as zirconium arsenate-modified magnetic
31 nanoparticles (ZrAs-Fe₃O₄@SiO₂) have been prepared for the enrichment of phosphorylated
32 peptides, which exploit the high affinity of positively charged metal cations to negatively charged
33 phosphorylated peptides [23]. The hydrazide-functionalized magnetic nanoparticles have been
34 fabricated for specific enrichment of glycosylated peptides [24,25]. Therefore, the functionalized
35 magnetic material has a broad application prospect in the life science.

36
37 Detonation nanodiamond (dND), with its prominent features of very small particle sizes
38 (3-10 nm), high surface area, chemical stability, biological compatibility, and non-toxicity is well
39 believed to be a promising material for biological applications. Especially, its high adsorption
40 capacity makes dNDs a good candidate for effective concentration and extraction of peptides and
41
42
43
44
45
46
47
48
49
50
51
52
53
54
55
56
57
58
59
60

1
2 proteins in dilute and contaminated sample [26-28]. However, dNDs are not easy to isolate and
3 tedious centrifugation steps are often required for further separation, which would limit its
4 analytical applications in the huge volume samples, such as the culture supernatant of cell. The
5 most advantage of magnetic microsphere is its super paramagnetic properties, which prevent the
6 magnetic microspheres from aggregating and enables them to re-disperse rapidly after the removal
7 of a magnetic field. Therefore, the combination of dNDs with magnetic microsphere will benefit
8 their further development, which will be an interesting advanced composite material as a result of
9 their strong sorption and super paramagnetic properties. It is worth noting that, in previous reports,
10 core-shell diamond particles were usually prepared by layer-by-layer (LbL) deposition on the
11 surface of diamond as a support for solid-phase extraction and high-performance liquid
12 chromatography. The core-shell particles shown significantly larger surface area than the original
13 solid particles and the highest efficiencies yet reported for a diamond-based chromatographic
14 support [29].

15
16 Thus, we fabricate a novel dND-functionalized magnetic silica microsphere
17 [Fe₃O₄@SiO₂@[dND]n] through layer-by-layer deposition of nanodiamond on magnetic silica
18 microsphere. While the novel materials maintaining excellent magnetic properties and admirable
19 adsorption, the process of enrichment is very fast, convenient and efficient. The novel material
20 was tested for their efficiency in the enrichment of the digestion of model proteins and a mixture
21 of model proteins. Moreover, the multiple functional groups outside of [Fe₃O₄@SiO₂@[dND]n]
22 played electrostatic interaction, hydrophilic and hydrophobic interaction with proteins in
23 biological sample. Thus it could be successfully applied to convenient, efficient and fast
24 enrichment of the secreted proteins in culture supernatant from human hepatoma cells.

25 26 27 28 29 30 31 32 33 34 35 36 37 38 39 40 41 42 43 44 45 46 47 48 49 50 51 52 53 54 55 56 57 58 59 60

2. Experiment

2.1 Reagents

Detonation nanodiamond was purchased from Gansu Lingyun Nanomaterial Corp. (Lanzhou, China). Proteins and reagents were purchased from Sigma-Aldrich (Mississauga, ON, Canada), including the following: bovine serum albumin (BSA), β-casein, cytochrome C (Cyto C), (3-aminopropyl)-triethoxysilane (APTEOS), poly-L-lysine hydrochloride (PL, molecular weight >18,000), 2-(N-morpholino) ethanesulfonic acid (MES), ammonium bicarbonate (NH₄HCO₃), glycine. 1-ethyl-3-(3-dimethylaminopropyl)-carbodiimide hydrochloride (EDC), N-hydroxysuccinimide (NHS) were purchased from Alfa Aesar (Ward Hill, MA, USA). Porcine trypsin was purchased from Promega (Madison, WI, USA). Analytical grade acetonitrile (ACN) and trifluoroacetic acid (TFA) were from Merck Millipore (Darmstadt, Germany). All of other chemicals were of analytical grade, and were purchased from Shanghai Chemical Reagent Co. (Shanghai, China). All reagents applied in SDS-electrophoresis were obtained from Bio-Rad (Hercules, CA, USA). Water used for all experiments was purified using a Milli-Q Plus system (Millipore, Bedford, MA, USA).

2.2 Synthesis of $\text{Fe}_3\text{O}_4@\text{SiO}_2@[\text{dND}]_n$ microspheres

Magnetic silica microspheres with a magnetite core of about 220 nm in diameter and silica shell of about 20 nm in thickness were synthesized according to our previous reported method [30]. After thoroughly washed with ethanol, 0.050 g of magnetic silica microspheres were dispersed in mixed solution of 160 mL ethanol, 40 mL deionized water and 5.0 mL APTEOS by ultrasonic vibration. Then, the obtained dispersion was subject to mechanical stirring at 40 °C, and 0.50 mL of ammonia aqueous solution were added into the dispersion with syringe. After stirring for 6 h, the resulting APTEOS-modified magnetic silica microspheres were recovered and washed with ethanol repeatedly.

dND particles were further carboxylated and oxidized with strong oxidative acid treatments following the procedure of Huang and Chang [31]. Carboxylic acid groups on the surface of heat- and acid-treated dND particles were activated by carbodiimide and subsequently reacted with NHS to provide a reactive site for covalent attachment to PL, as previously described [32,33]. dND particles (0.50 g) and 0.20 g of NHS were prepared in a 50 mM MES buffer solution (pH=6.1). Under the assistant of ultrasonic, 0.25 g of EDC was added quickly, and the mixture was continually stirred at room temperature for 1 h. The suspension was then centrifuged and rinsed thoroughly with MES buffer solution to remove excess EDC, NHS and byproduct urea.

0.25 g of APTEOS-modified magnetic silica microspheres and 0.05 g of the esterified dND particles were redispersed in 50 ml of MES buffer solution and then continually stirred for 1 h. The obtained dND-functionalized magnetic silica microspheres were separated with a magnet, washed with MES buffer solution by ultrasonic to remove any weakly adsorbed or unbound dND particles. Then, 0.10 wt% solution of PL was made from 0.050 g of PL powder in 50 mL of MES buffer solution, and 0.10 g of dND-functionalized magnetic silica microspheres was poured into this solution and stirred for 1 h to amine functionalize the outer surface of the dND particles in the first layer. The PL-dND functionalized magnetic silica microsphere was then washed extensively with ultrapure water. In the next step, the PL-dND functionalized magnetic silica microspheres was then poured into the suspension of the esterified dND particles as in the first deposition of dNDs. This general procedure was repeated until the desired number of PL-dND bilayers was deposited. At last, the final step was the block reaction of the unreacted epoxy groups of dND particles with 0.10 wt% solution of PL.

2.3 Characterization of $\text{Fe}_3\text{O}_4@\text{SiO}_2@[\text{dND}]_n$ microspheres

dND particles, $\text{Fe}_3\text{O}_4@\text{SiO}_2$ particles, $\text{Fe}_3\text{O}_4@\text{SiO}_2@d\text{NDs}$ particles, $\text{Fe}_3\text{O}_4@\text{SiO}_2@(\text{dNDs})_n$ particles were characterized by using Fourier transform infrared (FT-IR), respectively. FT-IR spectra were collected using a Nexus 470 FT-IR spectrometer (Nicolet, Madison, WI, USA). All samples were dehydrated before analysis. The size and morphology of $\text{Fe}_3\text{O}_4@\text{SiO}_2$ particles and $\text{Fe}_3\text{O}_4@\text{SiO}_2@(\text{dNDs})_n$ were observed using a JEOL model JEM-2011 (HR) transmission

1
2 electron microscope (TEM) (JEOL, Tokyo, Japan) at 200 kV, respectively. The mean size and
3 size distribution of the $\text{Fe}_3\text{O}_4@\text{SiO}_2@(\text{dNDS})_n$ were measured by dynamic light scattering (DLS)
4 (Malvern, Autoszer 4700) in aqueous solution with pH 4. All DLS measurements were carried out
5 with a wavelength of 532 nm at 25 °C and an angle detection of 90°.

8 9 **2.4 Pretreatment of standard peptides or proteins**

10 Suspension of $\text{Fe}_3\text{O}_4@\text{SiO}_2@[\text{dND}]_n$ microspheres (20.0 μL , 5 $\mu\text{g}/\mu\text{L}$) was added into a
11 solution (1.0 mL) containing certain concentrations of standard peptides or proteins. The solution
12 containing peptides or proteins and $\text{Fe}_3\text{O}_4@\text{SiO}_2@[\text{dND}]_n$ microspheres was shaken at room
13 temperature for 5 min. After decanting supernate with the help of magnet, the residue was rinsed
14 with water three times. And the peptides or proteins retained on the microsphere surface were
15 eluted with eluting solutions (50% ACN aqueous solution containing 0.1% TFA, 5.0 μL). The
16 elute containing the captured peptides or proteins was separated from $\text{Fe}_3\text{O}_4@\text{SiO}_2@[\text{dND}]_n$
17 microspheres with the help of magnet. The eluted procedure was repeated for better recovery of
18 peptides or proteins.

19 To evaluate the enrichment efficiency of $\text{Fe}_3\text{O}_4@\text{SiO}_2@[\text{dND}]_n$ microspheres for proteins, a
20 series of the mixed standard proteins were treated by $\text{Fe}_3\text{O}_4@\text{SiO}_2@[\text{dND}]_n$ microspheres. Then
21 the recovery and reproducibility of these proteins was investigated, which was the key factor for
22 the further application in real biological sample. BSA, Cyto C and β -casein were combined as the
23 standard protein mixture. The elute containing the captured proteins was separated and analyzed
24 by SDS-PAGE electrophoresis.

25 26 27 28 29 30 31 32 33 **2.5 Pretreatment of secretory proteins**

34 The human hepatoma cell line Huh-7 was cultured at 37 °C in 5% CO_2 in DMEM (Gibco,
35 USA) supplemented with 10% fetal bovine serum, 1% penicillin/streptomycin, and 1% glutamine
36 until approaching approximately 60-70% confluence. Cells were washed two times with PBS and
37 two times with serum- and phenol red-free DMEM cell medium. Cells were then incubated in the
38 serum- and phenol red-free cell medium at 37 °C. After 36 h, the culture supernatants containing
39 secreted proteins were collected and centrifuged at 1000 \times g for 5 min (4 °C) and subsequently
40 filtered using a 0.22 μm filter (Millipore, Bedford, MA, USA).

41 For the treatment of the culture supernatants from human hepatoma cells (10.0 mL), 0.50 mL
42 of suspension of $\text{Fe}_3\text{O}_4@\text{SiO}_2@[\text{dND}]_n$ microspheres was applied, and then shaken at 4 °C for 20
43 min. After the collection of magnetic microspheres by magnet, the supernatant was transferred and
44 treated with the same amount of $\text{Fe}_3\text{O}_4@\text{SiO}_2@[\text{dND}]_n$ nanoparticles again as mentioned above.
45 Then two parts of enriched microspheres were mixed and washed by 0.20 mL PBS buffer (pH, 7.4)
46 for three times. At last, the secreted proteins enriched on the microspheres were eluted by a series
47 of ACN aqueous solution (10%, 30% and 50%) for 5 min, and the combined elute was dried by
48 vacuum freeze-drying.

49 The enriched secreted proteins were dissolved in 50 mM NH_4HCO_3 buffer. Then trypsin was
50
51
52
53
54
55
56
57
58
59
60

1
2 added to the protein solution (1:30, w/w) and incubated at 37 °C overnight. The tryptic peptides
3 were fractionated on a Waters UPLC using a C18 column (BEH C18 2.1×50 mm, 1.7 μm, Waters,
4 Milford, MA, USA). Peptides were eluted at a flow rate of 600 μL/min with a linear gradient of
5 5–40% solvent B (ACN) over 15 min, the solvent A is 20mM ammonium formate with pH
6 adjusted to 10. The absorbance at 214 nm was monitored, and a total of 21 fractions were
7 collected. The fraction was separated by nano-HPLC (Eksigent Technologies, Redwood, CA, USA)
8 on the secondary reversed phase analytical column (C18, 3 μm, 150 mm×75 μm, Eksigent,
9 Redwood, CA, USA). Peptides were subsequently eluted using the following gradient conditions
10 with phase B (98% ACN/0.1% formic acid) from 5 to 45% B (5-100 min) and total flow rate was
11 maintained at 300 nL/min. Electrospray voltage of 2.5 kV versus the inlet of the Triple TOF 4600
12 mass spectrometer was used.

2.6 Mass spectrometry analysis

20 All MS analysis of standard peptides was performed on a 4700 Proteomics Analyzer
21 (TOF/TOF) (Applied Biosystems, Framingham, MA, USA). The instrument was operated at an
22 accelerating voltage of 20 kV. All mass spectra were obtained in the positive-ion reflection mode
23 with a mass range from 700 to 3200 Da and each spectrum was accumulated by 1000 laser shots
24 typically with automatic mode. Tryptic myoglobin peptides were used to calibrate the mass
25 instrument with an internal calibration mode. Mass accuracy was within 100 ppm. Mass spectral
26 data were examined and processed using Data Explorer 4.0 software supplied by Applied
27 Biosystems. GPS Explorer software (Applied Biosystems) with Mascot (Matrix Science, London,
28 UK) as a search engine was used to identify proteins. All standard proteins were identified using
29 the combination of PMF and MS/MS against Swiss-Prot database. The search parameters were set
30 up as follows: enzyme was trypsin, the number of missed cleavage sites was allowed up to 1, the
31 variable modification was oxidation of methionine, the mass tolerance of precursor ions and
32 fragments were 100 ppm and 0.2 Da, respectively.

33 Triple TOF 4600 mass spectrometer (Applied Biosystems, Framingham, MA, USA) was
34 operated in information-dependent data acquisition mode to switch automatically between MS and
35 MS/MS acquisition. MS spectra were acquired across the mass range of 350–1250 m/z using 250
36 ms accumulation time per spectrum. Tandem mass spectra scanned from 100–1250 m/z in high
37 sensitivity mode with rolling collision energy. The most intense precursors in the top of 25 were
38 selected for fragmentation per cycle with dynamic exclusion time of 25 s. Tandem mass spectra
39 were extracted and charge state de-convoluted by MS Data Converter from Applied Biosystems.
40 Database searches to identify the peptides were performed with Mascot (v.2.3, Matrix Science)
41 against the Swiss-Prot human database. The search parameters included the following: (i)
42 precursor ion mass tolerance less than 25 ppm; (ii) fragment ion mass tolerance less than 0.1 Da;
43 (iii) up to two missed cleavage sites allowed; (iv) variable modifications, oxidation (M, +15.9949).
44 In the database searching, Percolator was applied.

2.7 Bioinformatics analysis of secretory proteins

The theoretical *pI* and molecular weight of the identified proteins were exported by Mascot. Protein sequences were retrieved from the Uniprot database. The bioinformatical confirmation of secretory proteins was carried out as follows. SecretomeP (<http://www.cbs.dtu.dk/services/SecretomeP>) was used first to predict non-classical secretory proteins (with no signal-peptide and SecretomeP score >0.5) [34]. Then, the transmembrane hidden Markov model (TMHMM) algorithm (<http://www.cbs.dtu.dk/services/TMHMM>) was applied to map the putative transmembrane domains in the rest of proteins with confirmed signal peptide by SecretomeP [35]. The bio-functions of the identified proteins were analyzed with the Ingenuity Pathways Analysis (IPA, Ingenuity Systems, Mountain View, CA) [36].

3. Results and discussion

3.1 Preparation and characterization of $\text{Fe}_3\text{O}_4@\text{SiO}_2@(\text{dND})_n$

The overall synthetic procedure of $\text{Fe}_3\text{O}_4@\text{SiO}_2@(\text{dND})_n$ is illustrated in Scheme 1(a). Monodisperse Fe_3O_4 microspheres (~220 nm) were synthesized by using a solvothermal method, followed by coating with silica through a sol-gel process. After covalent grafting of APTES onto the silica-coated Fe_3O_4 , the functionalized Fe_3O_4 nanoparticles were readily grafted to the dNDs via covalent amide bonds. Meanwhile, the surface of dNDs was modified with a layer of PL. Then, one more layer of dND was assembled on the PL-functional dND-coated $\text{Fe}_3\text{O}_4@\text{SiO}_2$ through covalent bonds. This process was repeated until the core-shell particles contained five bilayers of PL-nanodiamond. Finally, the unreacted epoxy groups of dNDs on the microsphere surface were blocked with 0.10 wt% solution of PL. The product was denoted $\text{Fe}_3\text{O}_4@\text{SiO}_2@(\text{dND})_n$.

The newly synthesized materials were characterized by different techniques, including FT-IR and transmission electron microscopy (TEM). FT-IR was used to evaluate the preparation procedure. Fig. 1 shows the FT-IR spectra of dNDs, $\text{Fe}_3\text{O}_4@\text{SiO}_2$, $\text{Fe}_3\text{O}_4@\text{SiO}_2@(\text{dND})_n$ and $\text{Fe}_3\text{O}_4@\text{SiO}_2@(\text{dND})_n$, respectively. In the spectrum of dNDs (Fig. 1a), bands in the region 3424 cm^{-1} can be assigned to the surface hydroxyl O–H stretching vibrations of adsorbed water and/or surface carboxylic groups. $2850\text{--}2910\text{ cm}^{-1}$, 1676 cm^{-1} , and $1194\text{--}1112\text{ cm}^{-1}$ can be assigned to C–H stretching vibration, C=O stretching vibration, and C–O–C stretching vibration, respectively. In the spectrum of $\text{Fe}_3\text{O}_4@\text{SiO}_2$ (Fig. 1b), 1056 cm^{-1} and 570 cm^{-1} can be assigned to be Si–O–Si stretching vibration and Fe–O–Fe vibration. After the first deposition of dNDs on $\text{Fe}_3\text{O}_4@\text{SiO}_2$ particles (Fig. 1c), the intensity of the peak at $2850\text{--}2910\text{ cm}^{-1}$ ascribed to C–H stretch mode increased to some extent. In addition, the new peaks at 1634 cm^{-1} and 1542 cm^{-1} ascribed to carboxyl C=O stretch vibration of dNDs and/or PL and the stretching vibration of C–N also confirm the successful grafting of dNDs. In the spectra of $\text{Fe}_3\text{O}_4@\text{SiO}_2$ particles coated with 5 layers of dNDs (Fig. 1d), comparing with the intensity of the peaks ascribed to $-\text{CH}_2$ stretch vibration, C=O stretch vibration and C–N stretch vibration was increased slightly, which suggested that dNDs were successfully bonded on $\text{Fe}_3\text{O}_4@\text{SiO}_2$ particles surfaces via PL through a

1
2 layer-by-layer synthetic approach.

3
4 Fig. 2 presents the TEM images obtained from the core-shell structured magnetic silica
5 microspheres before (Fig. 2a) and (Fig. 2b, Fig.2c and Fig. 2d) after functionalized with dNDs.
6 Because the difference of density between Si and Fe is large, the black Fe₃O₄ particles had a
7 spherical shape with an average diameter of ~220 nm and were coated with an amorphous SiO₂
8 layer with the thickness of ~20 nm (Fig. 2a). As shown in Fig. 2b and 2c, after 5 times of coating
9 procedure with dNDs, the magnetic silica microspheres have been successfully functionalized
10 with uniform dNDs layers via PL. Although the Fe₃O₄@SiO₂@(dNDs)_n microspheres were
11 sonicated in ethanol before TEM measurements, the functionalized dNDs on microspheres was
12 stable, which also suggested dNDs were covalently bonded on Fe₃O₄@SiO₂@(dNDs)_n
13 microspheres surfaces via PL successfully. Furthermore, no free Fe₃O₄ nanoparticles or dNDs
14 were observed in Fig. 2d, indicating that the Fe₃O₄ nanoparticles, PL and dNDs have been
15 integrated into an entity. As shown in Fig. S1, it was also confirmed by dynamic light scattering
16 (DLS) that the hydrodynamic diameters for the Fe₃O₄@SiO₂@(dNDs)_n microspheres (619±80 nm)
17 increased by ~400 nm in comparison with those of the Fe₃O₄@SiO₂ particles (290±35 nm)
18 dispersed in aqueous solution. Meanwhile, it also proved that the Fe₃O₄@SiO₂@(dNDs)_n
19 microspheres has good dispersibility in aqueous solution, which might be valuable for the further
20 application in biological analysis. Together with the FTIR spectra, TEM images, and the
21 increasing size of Fe₃O₄@SiO₂@(dNDs)_n microspheres, these suggests that dNDs is indeed
22 covalent binding on magnetic particles via PL.
23

24
25 The synthesized Fe₃O₄@SiO₂@(dNDs)_n microspheres possess the super paramagnetic
26 properties, which can prevent the aggregation of microspheres. The microspheres display good
27 dispersibility in water or ethanol, which might be due to the numerous functional groups of dNDs
28 surfaces and the PL linkers. Additionally, it exhibits magnetic field-induced aggregation,
29 indicating fast response of magnetic microspheres in reply to magnetic field. It is found that the 80%
30 Fe₃O₄@SiO₂@(dNDs)_n microspheres could be separated from buffer solution easily with a magnet
31 in 15s (Supporting information Fig. S2). The excellent dispersion and super paramagnetic
32 properties make the novel layer-by-layer microspheres fascinating and promising for enrichment
33 of peptides and proteins in biological samples.
34

35 36 37 38 39 40 41 42 43 44 45 46 47 **3.2 Enrichment of standard peptides by Fe₃O₄@SiO₂@(dNDs)_n**

48
49 With a high surface area (400 m²/g) and abundant functional groups, dNDs provide an ideal
50 substrate for the enrichment of low abundant peptides [26]. In this study, the novel magnetic silica
51 nanoparticles functionalized with dNDs were prepared for the rapid and accessible pretreatment
52 approach. The collection efficiency of the composite materials also increased due to the magnetic
53 ferrite “core”. The performance of enrichment of peptides by Fe₃O₄@SiO₂@(dNDs)_n was
54 evaluated by the standard peptides of Lambinin B and tryptic digests of BSA. The enrichment
55 strategy was illustrated in Scheme 1b. After treatment by the novel microspheres, peptides were
56
57
58
59
60

1
2 eluted by ACN aqueous solution. Then, the elution could be either analyzed directly by
3 MALDI-MS or dried by vacuum freeze-drying for further MS analysis. The standard peptide of
4 Lambinin B (CDPGYLGSR, Mr 966.43) was applied for the evaluation of enriched equilibration
5 time by $\text{Fe}_3\text{O}_4@\text{SiO}_2@(\text{dNDs})_n$. The microspheres were incubated with standard peptides of
6 Lambinin B (0.50 fmol/ μL , 1 mL) for 2, 4, 6, 8, 10, 15, 25 and 30 min, respectively. After eluted
7 by 10 μL of 50% ACN aqueous solution containing 0.1% TFA for 5 min, 1 μL of elute was
8 analyzed by MALDI-TOF MS. The signal intensity percentage of peptide was measured with
9 respect to the different incubation time. As shown in Fig. S3, the enrichment saturates within 6
10 min and this value can be considered as the equilibrium time for the further peptide treatment. The
11 short equilibrium time is attributed to the significant interaction between the peptides and dNDs
12 on the microsphere surface as well as the PL linker.

13
14
15
16 To evaluate the enrichment capacity of the novel microspheres, 1 mL of tryptic digests of
17 BSA (from 1 to 50 fmol/ μL) was treated with 20 μg of $\text{Fe}_3\text{O}_4@\text{SiO}_2@(\text{dNDs})_n$ microsphere,
18 respectively. The tryptic digests of BSA enriched by the microspheres were eluted by 5.0 μL of 50%
19 ACN aqueous solution containing 0.1% TFA, and then 1 μL of elute was deposited on MALDI
20 stainless plate for MS analysis. Each concentration was repeated six times. Four typical tryptic
21 peptides of BSA, m/z at 927.5 (YLYEIAR), 1163.3 (LVNELTEFAK), 1479.6
22 (LGEYGFQNALIVR) and 1567.7 (DAFLGSFLYEYSR), were used for the enrichment isotherm.
23 As illustrated in Fig. 3, the average signal intensity of four peptides was enhanced from 304.9 to
24 2000.4 with the concentration of tryptic BSA peptides increased to 20 fmol/ μL and saturated with
25 further concentration. Attributed to the dNDs functionalized on magnetic particles and a much
26 larger surface area-to-mass ration of dNDs, the enrichment of peptides to the novel microspheres
27 saturated at 70 mg/g. Therefore, $\text{Fe}_3\text{O}_4@\text{SiO}_2@(\text{dNDs})_n$ microsphere has the potential to be a
28 good material for the enrichment of peptides in diluted sample solution.

29
30
31
32
33
34
35
36
37
38
39
40
41
42
43
44
45
46
47
48
49
50
51
52
53
54
55
56
57
58
59
60
61
62
63
64
65
66
67
68
69
70
71
72
73
74
75
76
77
78
79
80
81
82
83
84
85
86
87
88
89
90
91
92
93
94
95
96
97
98
99
100
101
102
103
104
105
106
107
108
109
110
111
112
113
114
115
116
117
118
119
120
121
122
123
124
125
126
127
128
129
130
131
132
133
134
135
136
137
138
139
140
141
142
143
144
145
146
147
148
149
150
151
152
153
154
155
156
157
158
159
160
161
162
163
164
165
166
167
168
169
170
171
172
173
174
175
176
177
178
179
180
181
182
183
184
185
186
187
188
189
190
191
192
193
194
195
196
197
198
199
200
201
202
203
204
205
206
207
208
209
210
211
212
213
214
215
216
217
218
219
220
221
222
223
224
225
226
227
228
229
230
231
232
233
234
235
236
237
238
239
240
241
242
243
244
245
246
247
248
249
250
251
252
253
254
255
256
257
258
259
260
261
262
263
264
265
266
267
268
269
270
271
272
273
274
275
276
277
278
279
280
281
282
283
284
285
286
287
288
289
290
291
292
293
294
295
296
297
298
299
300
301
302
303
304
305
306
307
308
309
310
311
312
313
314
315
316
317
318
319
320
321
322
323
324
325
326
327
328
329
330
331
332
333
334
335
336
337
338
339
340
341
342
343
344
345
346
347
348
349
350
351
352
353
354
355
356
357
358
359
360
361
362
363
364
365
366
367
368
369
370
371
372
373
374
375
376
377
378
379
380
381
382
383
384
385
386
387
388
389
390
391
392
393
394
395
396
397
398
399
400
401
402
403
404
405
406
407
408
409
410
411
412
413
414
415
416
417
418
419
420
421
422
423
424
425
426
427
428
429
430
431
432
433
434
435
436
437
438
439
440
441
442
443
444
445
446
447
448
449
450
451
452
453
454
455
456
457
458
459
460
461
462
463
464
465
466
467
468
469
470
471
472
473
474
475
476
477
478
479
480
481
482
483
484
485
486
487
488
489
490
491
492
493
494
495
496
497
498
499
500
501
502
503
504
505
506
507
508
509
510
511
512
513
514
515
516
517
518
519
520
521
522
523
524
525
526
527
528
529
530
531
532
533
534
535
536
537
538
539
540
541
542
543
544
545
546
547
548
549
550
551
552
553
554
555
556
557
558
559
560
561
562
563
564
565
566
567
568
569
570
571
572
573
574
575
576
577
578
579
580
581
582
583
584
585
586
587
588
589
590
591
592
593
594
595
596
597
598
599
600
601
602
603
604
605
606
607
608
609
610
611
612
613
614
615
616
617
618
619
620
621
622
623
624
625
626
627
628
629
630
631
632
633
634
635
636
637
638
639
640
641
642
643
644
645
646
647
648
649
650
651
652
653
654
655
656
657
658
659
660
661
662
663
664
665
666
667
668
669
670
671
672
673
674
675
676
677
678
679
680
681
682
683
684
685
686
687
688
689
690
691
692
693
694
695
696
697
698
699
700
701
702
703
704
705
706
707
708
709
710
711
712
713
714
715
716
717
718
719
720
721
722
723
724
725
726
727
728
729
730
731
732
733
734
735
736
737
738
739
740
741
742
743
744
745
746
747
748
749
750
751
752
753
754
755
756
757
758
759
760
761
762
763
764
765
766
767
768
769
770
771
772
773
774
775
776
777
778
779
780
781
782
783
784
785
786
787
788
789
790
791
792
793
794
795
796
797
798
799
800
801
802
803
804
805
806
807
808
809
810
811
812
813
814
815
816
817
818
819
820
821
822
823
824
825
826
827
828
829
830
831
832
833
834
835
836
837
838
839
840
841
842
843
844
845
846
847
848
849
850
851
852
853
854
855
856
857
858
859
860
861
862
863
864
865
866
867
868
869
870
871
872
873
874
875
876
877
878
879
880
881
882
883
884
885
886
887
888
889
890
891
892
893
894
895
896
897
898
899
900
901
902
903
904
905
906
907
908
909
910
911
912
913
914
915
916
917
918
919
920
921
922
923
924
925
926
927
928
929
930
931
932
933
934
935
936
937
938
939
940
941
942
943
944
945
946
947
948
949
950
951
952
953
954
955
956
957
958
959
960
961
962
963
964
965
966
967
968
969
970
971
972
973
974
975
976
977
978
979
980
981
982
983
984
985
986
987
988
989
990
991
992
993
994
995
996
997
998
999
1000

Generally, real biological samples always contain salts, or other contaminants for the maintenance of a non-toxic environment for cells, stabilization of solvated sample and other biological activity. However, these salts, or other contaminants play a strong negative effect on the quality of mass spectrometry analysis and can even completely suppress the signals of MS. Therefore, a desalting or accessional step is necessary after conventional pretreatment processes. The previous reports have revealed that the potential of using dNDs as an adsorbent for desalting and subsequent MALDI-MS analysis. In the present study, we also explored the power of $\text{Fe}_3\text{O}_4@\text{SiO}_2@(\text{dNDs})_n$ for desalting. In the presence of saturated NaCl solution, a mass spectrum with high quality of 1 μL of tryptic BSA peptides (2 fmol/ μL) can hardly be obtained (Fig. 4a). The peptide signals were greatly suppressed by the high concentration of salts. When the identical sample was pretreated by the novel microspheres, peptides can be captured on the layer-by-layer dNDs outside the silica-coated ferrite “core” by hydrophobic interaction and other molecular interaction. Then the salt was washed by aqueous solution. After the elution with 50% ACN

aqueous solution containing 0.1% TFA, a very clear peptide fingerprinting was observed with highly enhanced signals (Fig. 4b). It can be safe to draw the conclusion that $\text{Fe}_3\text{O}_4@\text{SiO}_2@(\text{dNDS})_n$ has good salt tolerance capability. Therefore, with the aid of silica-coated ferrite “core”, the easy separation of target-molecule-bound nanoparticles using an external magnetic field and the powerful salt tolerance capability make the novel microspheres easy and powerful for pretreatment of peptides in diluted and complicated sample.

3.3 Enrichment of standard proteins by $\text{Fe}_3\text{O}_4@\text{SiO}_2@(\text{dNDS})_n$

To examine the recovery and reproducibility of $\text{Fe}_3\text{O}_4@\text{SiO}_2@(\text{dNDS})_n$ microspheres in low-abundance protein enrichment, a mixture of model protein (S) including BSA (3 $\mu\text{g}/\text{mL}$), β -casein (2 $\mu\text{g}/\text{mL}$) and Cyto C (5 $\mu\text{g}/\text{mL}$) was used. Fig. 5a displays the silver stained SDS-PAGE of standard proteins with a series of varying amounts from 0.2S to 4S. The amount of BSA, β -casein and Cyto C in 1S sample is 0.75 μg , 0.5 μg and 1.25 μg , respectively. Quantity analysis of each standard protein in SDS-PAGE gel was performed by Quantity One software (Version 4.3, Bio-Rad Laboratories). As shown in Fig. S4, the amount of each standard protein versus the gray value of each lane gives good linearity, such as $y=54.62\ln(x)+192.92$, $R^2=0.93$ (BSA, MW= 69 248Da, $pI=5.83$), $y=47.34\ln(x)+88.99$, $R^2=0.98$ (β -casein, MW=23 583Da, $pI=5.13$) and $y=87.03\ln(x)+184.49$, $R^2=0.96$ (Cyto C, MW=11 832Da, $pI= 9.59$). After incubated in 1 mL of the mixed standard protein BSA (3 $\mu\text{g}/\text{mL}$), β -casein (2 $\mu\text{g}/\text{mL}$) and Cyto C (5 $\mu\text{g}/\text{mL}$) for 6 min, 300 μg $\text{Fe}_3\text{O}_4@\text{SiO}_2@(\text{dNDS})_n$ microspheres were sequential resuspended in the elution buffer (20% ACN aqueous solution containing 0.1% TFA and 50% ACN aqueous solution containing 0.1% TFA). Each elution was vacuum dried and then separated under the same SDS-page condition, respectively (Fig. 5b and Fig. 5c). To evaluate the reproducibility of the novel pretreatment approach for proteins, the enriching procedure was repeated five times, respectively. As calculated by the linearity of gray value with the amount of standard proteins, the recovery of each protein summed by two SDS-page is $93(\pm 2.03)\%$, $99(\pm 2.93)\%$, $89(\pm 2.25)\%$, respectively. Based on these results, the novel $\text{Fe}_3\text{O}_4@\text{SiO}_2@(\text{dNDS})_n$ microsphere is of good practical values in that it displays high enrichment efficiency in the enrichment of low-abundance peptides or proteins. After regeneration of protein, the TEM image of $\text{Fe}_3\text{O}_4@\text{SiO}_2@(\text{dNDS})_n$ (Fig. S5) shows the stability of the functionalized dNDS outside microspheres as the former one (Fig. 2c). Thus, the functionalized magnetic microsphere has the capability for re-use.

In the synthesis of the novel magnetic microspheres, PL was used as blocking agent to stop layer-by-layer deposition of dNDS. Thus, the outer-layer of the $\text{Fe}_3\text{O}_4@\text{SiO}_2@(\text{dNDS})_n$ microspheres shows positive charges under the incubation buffer (Tris-HCl, pH 7.4). Meanwhile, the BSA and β -casein carry negative charges in the same conditions due to their theoretical pI values of BSA and β -casein are about 5.0. Owing to the electrostatic interactions between negative charge of model proteins and positive charge of PL, the novel microspheres can be applied in the enrichment of BSA and β -casein efficiently. Because the electrostatic interactions

1
2 can be easily broken in the low concentration of organic solvent eluent, the model proteins of BSA
3 and β -casein were easier eluted than that of Cyto C in 20% ACN aqueous solution containing 0.1%
4 TFA (Fig. S4b). However, the functional group of dND shows high hydrophilic and hydrophobic
5 interaction between the novel microspheres and proteins. Even though it carries positive charges at
6 pH 7.4, Cyto C ($pI=9.59$) can also be enriched by the hydrophilic/hydrophobic interactions. In Fig.
7 S4c, the Cyto C can be totally eluted in the high concentration organic solvent eluent. Therefore,
8 the mechanism of the novel microspheres for enrichment of proteins is complex interaction of
9 electrostatic interaction, hydrophilic and hydrophobic interaction.
10

11 3.4 Application to secretome analysis

12 To intensively evaluate the feasibility of the magnetic microspheres for the secreted protein
13 enrichment, this material was further applied to complex biological samples. Cancer cell
14 secretome profiling has been shown to be a promising strategy for identifying potential cancer
15 biomarkers. In this study, $Fe_3O_4@SiO_2@[dND]_n$ microspheres were used to capture secreted
16 proteins in Huh-7 cells, followed by separation and detection using 2-D LC/ESI-MS/MS. As a
17 result, a total of 1473 unique proteins were identified with duplicate experiments.
18

19 The identified proteins were further analyzed using bioinformatics programs designed to
20 predict protein secretion pathways. Among the identified 1473 proteins, 611 proteins were
21 predicted to be secreted in the classical secretory pathway based on the presence of a signal
22 peptide and the absence of transmembrane domains by SecretomeP program and TMHMM. And
23 409 proteins were verified to be secretory proteins released through non-classical secretory
24 pathway by the SecretomeP program. Additionally, 132 proteins were determined by TMHMM
25 algorithm as membrane secretory proteins but could be categorized as neither classical nor
26 non-classical secretion [15]. Collectively, 50.4% (743/1473) of the identified proteins can be
27 verified as secretory proteins by these analyses, and this ratio is consistent with previous studies
28 [37].
29

30 The MW, pI (Isoelectric point), GRAVY (the grand average of hydropathicity) of each
31 protein was then investigated to examine the universality of our method. As a result, the 1473
32 identified proteins showed a wide MW distribution (Fig. 6a) and a broad pI distribution (Fig. 6b)
33 even including very basic proteins (up to pI 12.24). Among them, the percentage of the proteins
34 with MW below 30 kDa reaches 25.6% (377/1473). Many of the identified LMWPs (low
35 molecular weight proteins) are known to be associated with cancer development and metastasis,
36 such as platelet-derived growth factor subunit B (PDGFB), neurotensin/neuromedin N (NEUT),
37 extracellular superoxide dismutase [Cu-Zn] (SODC), etc [38-41]. As shown in Fig. S6 shows the
38 distribution of GRAVY of the secreted proteins in Huh-7 cells enriched by $Fe_3O_4@SiO_2@[dND]_n$
39 microspheres, the GRAVY of the mostly classical secretory proteins and non-classical secretory
40 proteins bellows zero. The most secretory proteins enriched in the culture supernatant from Huh-7
41 cell were hydrophilic protein matched with the characteristic of secretory protein. Thus, the above
42
43
44
45
46
47
48
49
50
51
52
53
54
55
56
57
58
59
60

1
2 results show the high efficiency and universality of this method. The detailed information on all
3 proteins identified including the Swiss-Prot accession names, MW, pI, etc. is provided in
4 Supporting Information Table S1.
5

6
7 The bio-functions of the identified proteins were further analyzed with the IPA tool (Fig. S7)
8 Major functions of the identified secreted proteins are “Cellular Growth and Proliferation”, “Cell
9 Death and Survival”, “Protein Synthesis”, “Infections Disease” and “Cellular Movement”. These
10 bio-functions are reported to play important roles in the development and invasion of cancer
11 [42-44]. And these observations support the viewpoint that the secretome of cancer cells
12 represents an attractive pool for biomarker discovery.
13

14
15 Some well-known hepatocellular carcinoma biomarkers such as alpha fetoprotein (AFP),
16 apolipoprotein E (APOE), osteopontin (OPN) and dickkopf-related protein 1 (DKK1) were
17 identified in this study [45-47]. In addition, some proteins included in our list were scarcely
18 identified in previous studies of HCC-derived secretome, such as EGF-like repeat and discoidin
19 I-like domain-containing protein 3 (EDIL3), NEUT, and bone morphogenetic protein 4 (BMP4),
20 which show high efficiency of the novel material for the secreted protein enrichment [48-50].
21 Moreover, these proteins are found to be involved in the development, prognosis and treatment of
22 HCC. It was reported that high levels of autocrine EDIL3 may contribute to the receptive
23 microenvironment for the survival of detached HCC cells and may involve in cancer cell
24 spreading [51,52]. Dysfunctional activation of the NEUT/IL-8 pathway was detected in HCC
25 which is associated with increased inflammatory response in microenvironment, enhanced
26 epithelial mesenchymal transition in cancer, and worse prognosis in HCC patients [39]. BMP4
27 signaling was previously shown to play a critical role in the differentiation of cancer stem cells
28 and might be a potent therapeutic agent in HCC [53]. These results further underscore the value of
29 $\text{Fe}_3\text{O}_4@\text{SiO}_2@[\text{dND}]_n$ microspheres in secreted proteins enrichment and analysis.
30
31

32 4. Conclusions

33
34 In summary, magnetic $\text{Fe}_3\text{O}_4@\text{SiO}_2@[\text{dND}]_n$ microspheres were prepared and applied for
35 the first time in enrichment and desalting of low-abundance of peptides and proteins. Due to the
36 high absorption capacity of dNDs for biomolecules, the novel magnetic microspheres showed the
37 excellent performance in concentration of peptides and proteins in highly diluted and complicated
38 samples. The enrichment process was fast and efficient. Furthermore, the successful application of
39 $\text{Fe}_3\text{O}_4@\text{SiO}_2@[\text{dND}]_n$ in the direct harvesting of secreted proteins from large sample volumes
40 demonstrated it is a promising tool for proteomics and secretome research.
41

42 Acknowledgements

43
44 The authors acknowledge the financial support from the MOST 973/863 program (No.
45 2011CB910604, 2012AA020200), National NSF (No. 21305018, 20975024, 20735005, 30672394
46 and 30530040), Science and Technology Commission of Shanghai Municipality under Grant (No.
47 15DZ2291100), Shanghai Leading Academic Discipline (No. B109), RFDP (No.
48
49
50
51
52
53
54
55
56
57
58
59
60

20130071140007), CERS-1-66 and Shanghai Key Lab of Forensic Medicine (No. KF1404).

References

- [1] Stastna M., Van Eyk J. E., *Proteomics* 2012, 12, 722-735.
- [2] Pavlou M.P., Diamandis E.P., *J Proteomics* 2010, 73, 1896-1906.
- [3] Tarassishin L., Lim J., Weatherly D. B., Angeletti R. H., Lee S. C., *J. Proteomics* 2014, 99, 152-168.
- [4] Lee Y. C., Gajdosik M. S., Josic D., Clifton J. G., Logothetis C., Yu-Lee L. Y., Gallick G. E., Maity S. N., Lin S. H., *Mol. Cell Proteomics* 2015, 14, 471-483.
- [5] Mbeunkui F., Fodstad O., Pannell L.K., *J. Proteome Res.* 2006, 5, 899-906.
- [6] Ray S., Chandra H., Srivastava S., *Biosens. Bioelectron.* 2010, 25, 2389-2401.
- [7] Chen X., Wang X., Liu L., Yang D., Fan L., *Anal. Chim. Acta*, 2005, 542, 144-150.
- [8] Shen W., Xiong H., Xu Y., Cai S., Lu H., Yang P., *Anal. Chem.* 2008, 80, 6758-6763.
- [9] Xiong H., Guan X., Jin L., Shen W., Lu H., Xia Y., *Angew. Chem. Int. Ed.* 2008, 47, 4204-4207.
- [10] Viñas P., Campillo N., Martínez-Castillo N., Hernández-Córdoba M., *J. Chromatogr. A* 2009, 1216, 1279-1284.
- [11] Tian R., Zhang H., Ye M., Jiang X., Hu L., Bao X., Zou H., *Angew. Chem. Int. Ed.* 2007, 46, 962-965.
- [12] Jia W., Chen X., Lu H., Yang P., *Angew. Chem. Int. Ed.* 2006, 45, 3345-3349.
- [13] Shriver-Lake L.C., Gammeter W.B., Bang S.S., Pazirandeh M., *Anal. Chim. Acta* 2002, 470, 71-78.
- [14] Ye N., *Anal. Lett.* 2008, 41, 2554-2563.
- [15] Cao J., Hu Y.Y., Shen C.P., Yao J., Wei L.M., Yang F.Y., Nie A.Y., Wang H., Shen H.L., Liu Y.K., Zhang Y.H., Tang Y., Yang P.Y., *Proteomics* 2009, 9, 4881-4888.
- [16] Paule S., Meehan K., Czuk A. R., Stephens A. N., Nie G.Y., *Proteome Sci.* 2011, 9, 50.
- [17] Zhao M., Xie Y., Deng C., Zhang X., *J. Chromatogr. A* 2014, 1357, 182-193.
- [18] Chen H., Deng C., Zhang X., *Angew. Chem. Int. Ed Engl.* 2010, 49, 607-611.
- [19] Liu S., Li Y., Deng C., Mao Y., Zhang X., Yang P., *Proteomics* 2011, 11, 4503-4513.
- [20] Chen H., Qi D., Deng C., Yang P., Zhang X., *Proteomics* 2009, 9, 380-387.
- [21] Liu Q., Shi J., Cheng M., Li G., Gao D., Jiang G., *Chem. Commun.* 2012, 48, 1874-1876.
- [22] Shi C., Meng J., Deng C., *Chem. Commun.* 2012, 48, 2418-2420.
- [23] Li X.S., Xu L.D., Zhu G.T., Yuan B.F., Feng Y.Q., *Analyst*, 2012, 137, 959-967.
- [24] Cao Q., Ma C., Bai H., Li X., Yan H., Zhao Y., Ying W., Qian X., *Analyst*, 2014, 139, 603-609.
- [25] Huang G., Sun Z., Qin H., Zhao L., Xiong Z., Peng X., Ou J., Zou H., *Analyst*, 2014, 139, 2199-2206.
- [26] Wei L., Shen Q., Lu H., Yang P., *J. Chromatogr. B* 2009, 877, 3631-3637.
- [27] Pham M. D., Yu S.F., Han C. C., Chan S. I., *Anal. Chem.* 2013, 85, 6748-6755.
- [28] Wei L. M., Xue Y., Zhou X. W., Jin, H. Shi Q., Lu H. J., Yang P. Y., *Talanta* 2008, 74, 1363-1370.

- 1
2 [29] Saini G., Jensen D. S., Wiest L. A., Vail M. A., Dadson A., Lee M. L., Shutthanandan V.,
3 Linford M. R., *Anal. Chem.* 2010, 82, 4448-4456
4
5 [30] Zhou W., Yao N., Yao G., Deng C., Zhang X., Yang P., *Chem. Commun.* 2008, 43, 5577-5579.
6
7 [31] Huang L. C. L., Chang H. C., *Langmuir.* 2004, 20, 5879-5884.
8
9 [32] Huang W.J., Taylor S., Fu K.F., Zhang D.H., Hanks T.W., Rao A.M., Sun Y.P., *Nano Lett.*
10 2002, 2, 311-314.
11
12 [33] Wong S.S., Woolley A.T., Joselevich E., Cheung C.L., Lieber C.M., *J. Am. Chem. Soc.* 1998,
13 120, 8557-8558.
14
15 [34] Bendtsen J. D., Jensen L. J., Blom N., Von Heijne G, Brunak S., *Protein Eng. Des. Sel.* 2004,
16 17, 349-356.
17
18 [35] Krogh A., Larsson B., Heijne G., Sonnhammer E. L. L., *J. Mol. Biol.* 2001, 305, 567-580.
19
20 [36] Yu Y., Shen H., Yu H., Zhong F., Zhang Y., Zhang C., Zhao J., Li H., Chen J., Liu Y., Yang P.,
21 *Mol. BioSyst.*, 2011, 7, 1908-1916.
22
23 [37] Wu C. C., Cheng H. C., Chen S. J., Liu H. P., Hsieh Y. Y., Yu C. J., Tang R., Hsieh L. L., Yu J.
24 S., Chang Y. S., *Proteomics* 2008, 8, 316-332.
25
26 [38] Slattery M.L., John E. M., Stern M. C., Herrick J., Lundgreen A., Giuliano A. R., Hines L.,
27 Baumgartner K. B., Torres-Mejia G., Wolff R. K., *Breast Cancer Res. Treat* 2013, 140, 587-601.
28
29 [39] Yu J.P., Ren X.B., Chen Y.Z., Liu P.P., Wei X.Y., Li H., Ying G.G., Chen K.X., Winkler H.,
30 Hao X.S., *Plos one* 2013, 8, e56069.
31
32 [40] Tang K. H., Ma S., Lee T.K., Chan Y. P., Kwan P. S., Tong C. M., Ng I. O., Man K., To K.F.,
33 Lai P. B., Lo C. M., Guan X. Y., Chan K. W., *Hepatology* 2012, 55, 807-820.
34
35 [41] Kim J., Mizokami A., Shin M., Izumi K., Konaka H., Kadono Y., Kitagawa Y., Keller E.T.,
36 Zhang J., Namiki M., *Anticancer Res.* 2014, 34, 2821-2832.
37
38 [42] Al-Mehdi A. B., Tozawa K., Fisher A. B., Shientag L., Lee A., Muschel, R. J., *Nat. Med.* 2000,
39 6, 100-102.
40
41 [43] Jaattela M., *Exp. Cell Res.* 1999, 248, 30-43.
42
43 [44] Kang Y., Massague J., *Cell* 2004, 118, 277-279.
44
45 [45] Wan H.G., Xu H., Gu Y.M., Wang H., Xu W., Zu M.H., *Clin. Res. Hepatol. Gas.* 2014, 38,
46 706-714.
47
48 [46] Yokoyama Y., Kuramitsu Y., Takashima M., *Int. J. Oncol.* 2006, 28, 625-631.
49
50 [47] Shen Q., Fan J., Yang X.R., Tan Y., Zhao W., *Lancet Oncol.* 2012, 13, 817-826.
51
52 [48] Wu C.C., Hsu C.W., Chen C.D., Yu C.J., Chang K.P., Tai D. I., Liu H. P., Su W.H., Chang Y.
53 S., Yu J. S., *Mol. Cell. Proteomics* 2010, 9, 1100-1117.
54
55 [49] Yamashita R., Fujiwara Y., Ikari K., Hamada K., Otomo A., Yasuda K., Noda M., Kaburagi Y.,
56 *Mol. Cell. Biochem.* 2007, 298, 83-92.
57
58 [50] Zwickl H., Traxler E., Staettner S., Parzefall W., Bettina G.K., Josef K., Rolf S.H.,
59 Christopher G., *Electrophoresis* 2005, 26, 2779-2785.
60
61 [51] Feng M.X., Ma M. Z., Fu Y., Li J., Wang T., Xue F., Zhang J.J., Qin W.X., Gu J.R., Zhang
Z.G., Xia Q., *Mol. Cancer* 2014, 13, 226-242.
62
63 [52] Sun J.C., Liang X.T., Pan K., Wang H., Zhao J.J., Li J.J., Ma H.Q., Chen Y.B., Xia J.C.,

1
2 *World J. Gastroenterol.* 2010, 16, 4611-4615.

3 [53] Zhang L.X., Sun H.F., Zhao F.Y., Lu P., Ge C., Li H., Hou H.L., Yan M.X., Chen T.Y., Jiang
4 G.P., Xie H.Y., Cui Y., Huang X.W., Fan J., Yao M., Li J.J., *Cancer Res.* 2012, 72, 4276-4285.
5
6
7
8

9
10 **Scheme 1.** Schematic illustrating the facile synthesis of novel magnetic silica nanoparticles
11 functionalized with dNDs by poly-L-lysine via a process of diimide-activated amidation (a), and its
12 application to the pretreatment of peptides and proteins in sample (b).
13
14

15
16 **Fig. 1.** FT-IR spectra of (a) dND particles, (b) $\text{Fe}_3\text{O}_4@\text{SiO}_2$ particles, (c) $\text{Fe}_3\text{O}_4@\text{SiO}_2@\text{dNDs}$
17 particles, and (d) $\text{Fe}_3\text{O}_4@\text{SiO}_2@(\text{dNDs})_n$ particles.
18
19

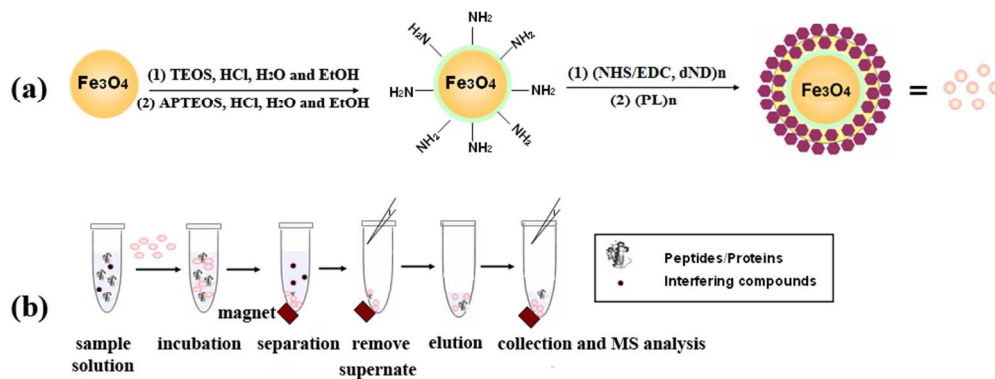
20
21 **Fig. 2.** TEM images of core-shell structured magnetic silica microspheres before (a) and after (b),
22 (c), (d) functionalized with dNDs.
23
24

25
26 **Fig. 3.** Enrichment isotherm of the tryptic BSA peptides pretreated by $\text{Fe}_3\text{O}_4@\text{SiO}_2@(\text{dNDs})_n$
27 particles. The m/z of tryptic BSA peptides are 927.5 (YLYEIAR), 1163.3 (LVNELTEFAK),
28 1479.6 (LGEYGFQNALIVR) and 1567.7 (DAFLGSFLYEYSR).
29
30

31
32 **Fig. 4.** MALDI-TOF mass spectrometry of 2 fmol/ μL tryptic BSA peptides (1 mL) in the presence
33 of saturated NaCl solution (a) without any pretreatment and (b) pretreated by
34 $\text{Fe}_3\text{O}_4@\text{SiO}_2@(\text{dNDs})_n$ (10 μg). (The asterisks in mass spectra denote peptides which can be
35 identified in database.)
36
37
38

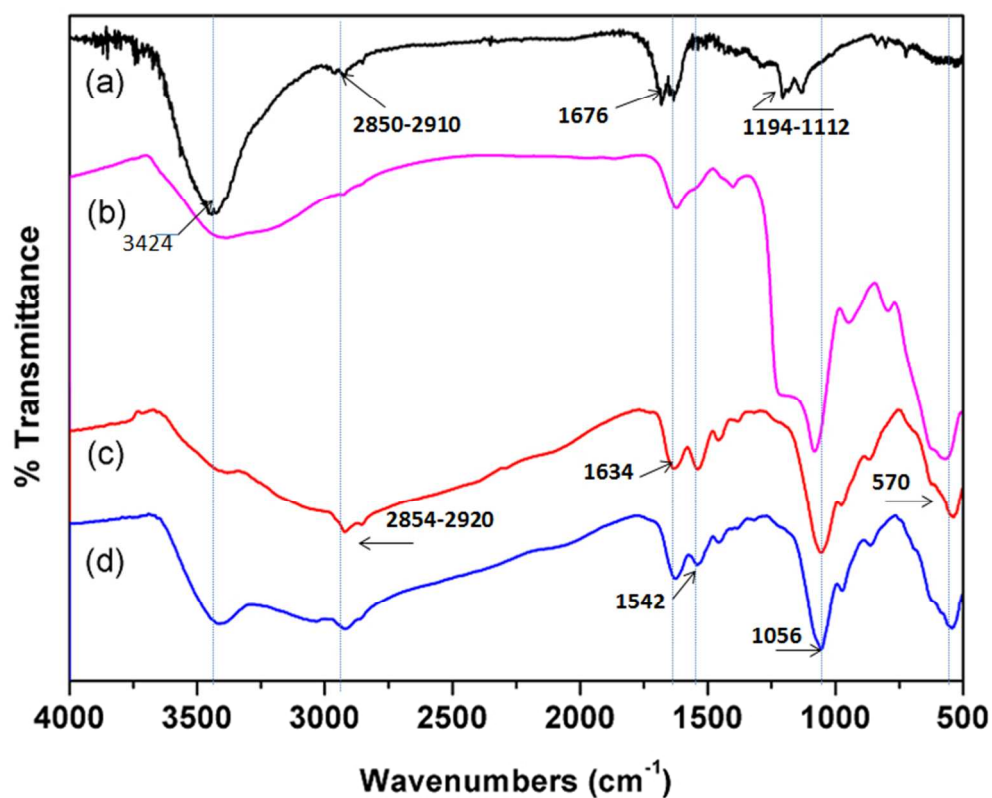
39
40 **Fig. 5.** SDS-PAGE analysis of the mixture of standard protein (BSA, β -casein and Cyto C). (a)
41 directly analysis of standard protein with a series of mixture protein 0.2S (L1), 0.4S (L2), 0.6S
42 (L3), 0.8S (L4), 1.0S (L5), 2.0S (L6), 4.0S (L7), respectively. The amount of BSA, β -casein and
43 Cyto C in 1S sample is 0.75 μg , 0.5 μg and 1.25 μg , respectively. (b) analysis of the mixture of
44 proteins eluted from $\text{Fe}_3\text{O}_4@\text{SiO}_2@(\text{dNDs})_n$ microsphere pretreated in the 1 mL of 4.0S sample
45 sequentially by 20% ACN aqueous solution containing 0.1% TFA and (c) 50% ACN aqueous
46 solution containing 0.1% TFA. To evaluate the recovery and reproducibility of the novel
47 enrichment approach, the process of the method repeated 5 times.
48
49
50
51
52

53
54 **Fig. 6.** Distribution of MW (a) and pI (b) of the secreted proteins in Huh-7 cells pretreated by
55 $\text{Fe}_3\text{O}_4@\text{SiO}_2@(\text{dNDs})_n$ particles.
56
57
58
59
60

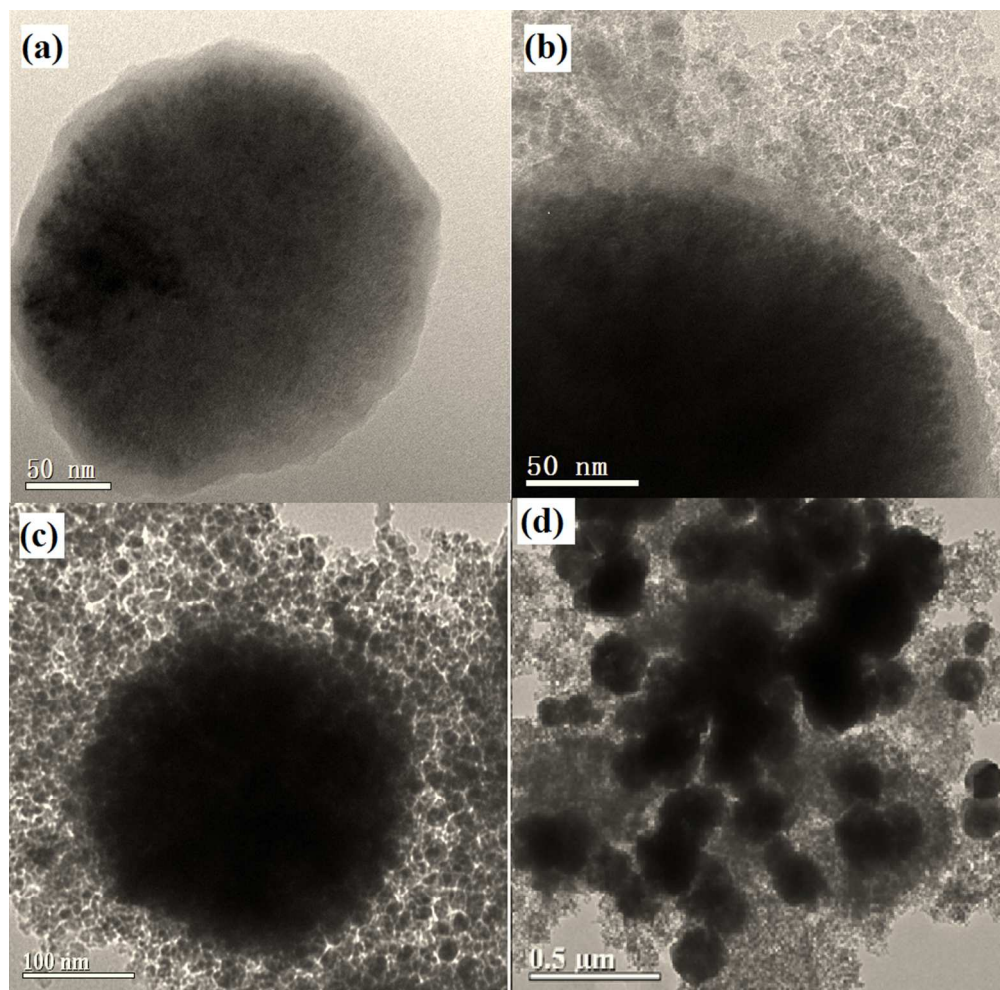


Schematic illustrating the facile synthesis of novel magnetic silica nanoparticles functionalized with dNDs by poly-L-lysine via a process of diimide-activated amidation (a), and its application to the pretreatment of peptides and proteins in sample (b).

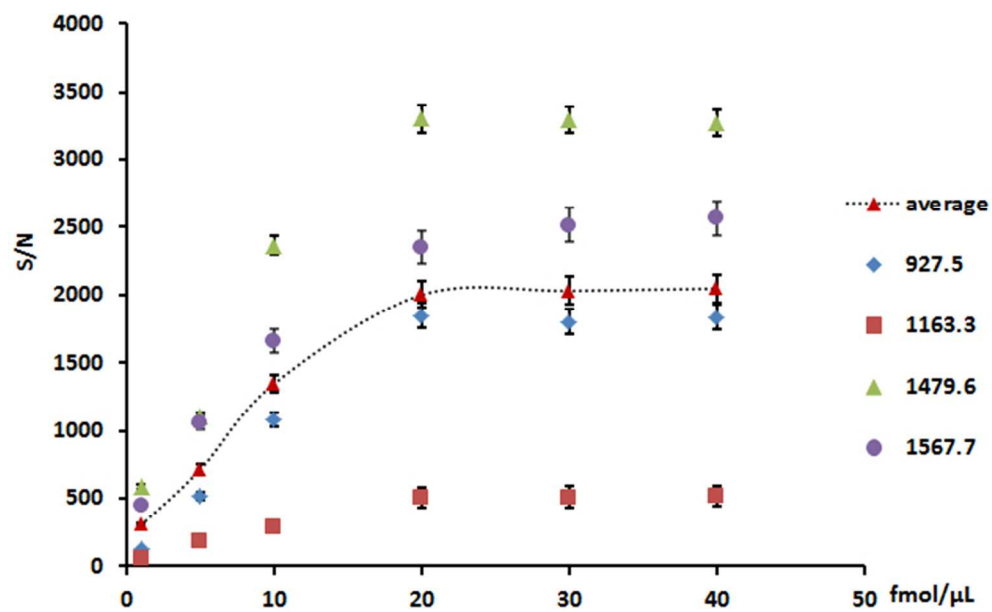
268x103mm (96 x 96 DPI)



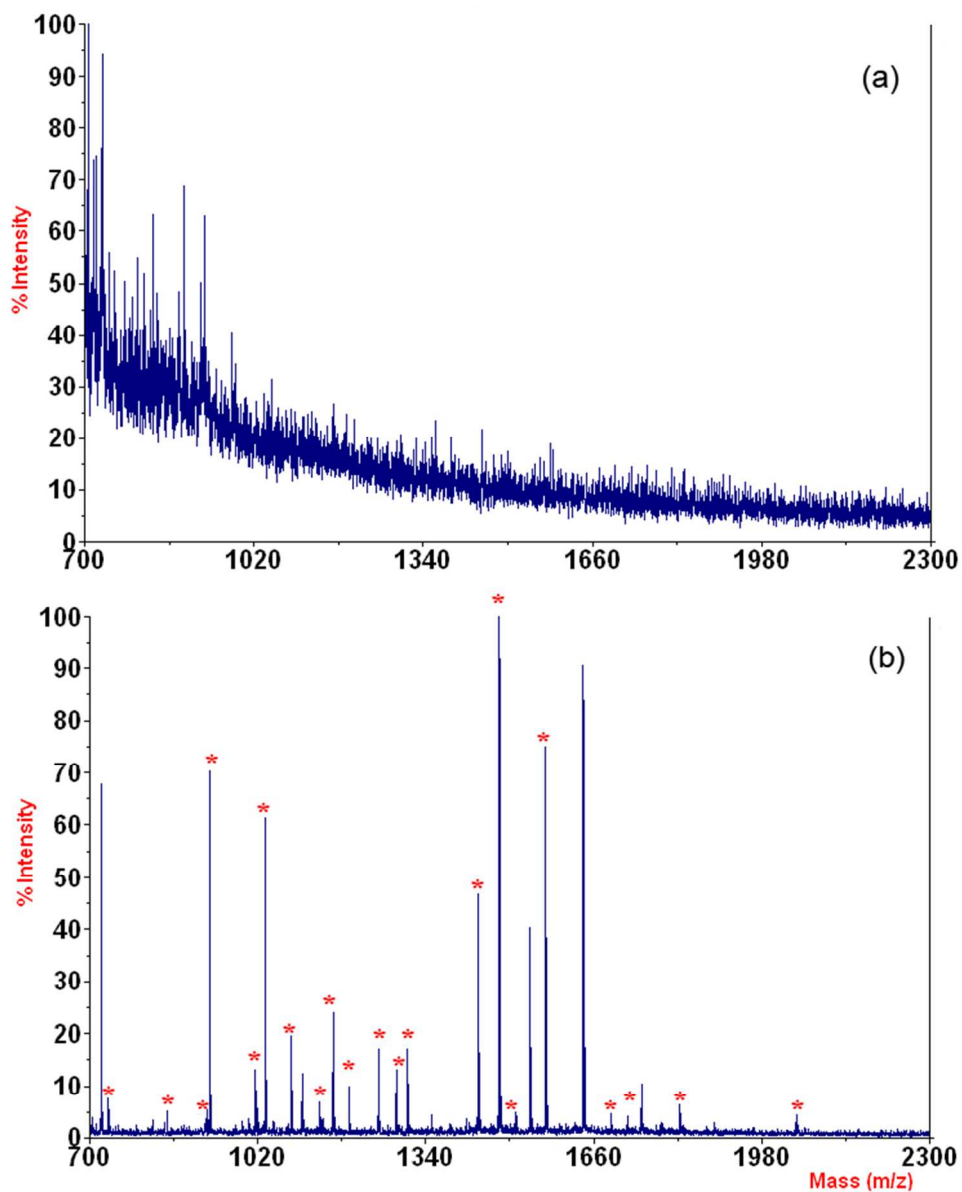
FT-IR spectra of (a) dND particles, (b) Fe₃O₄@SiO₂ particles, (c) Fe₃O₄@SiO₂@dNDs particles, and (d) Fe₃O₄@SiO₂@(dNDs)_n particles.
208x167mm (96 x 96 DPI)



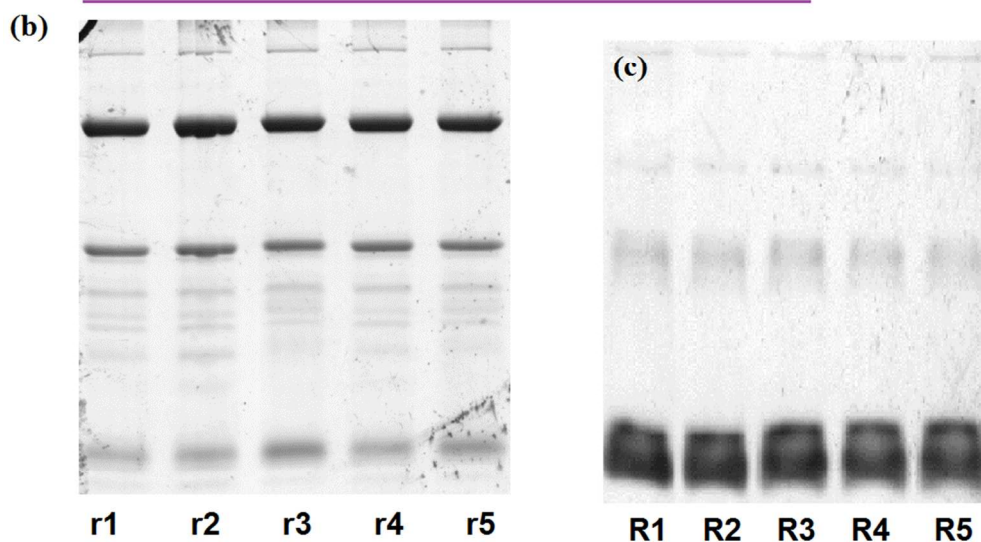
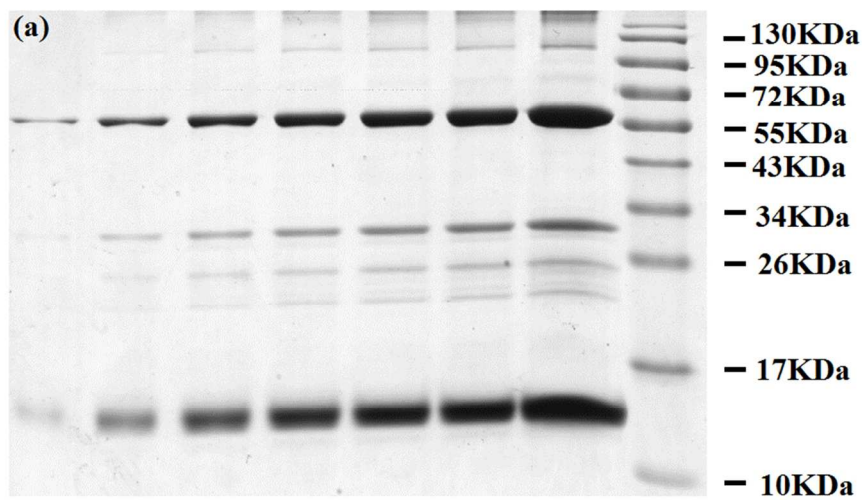
TEM images of core-shell structured magnetic silica microspheres before (a) and after (b), (c), (d) functionalized with dNDs.
270x266mm (96 x 96 DPI)



Enrichment isotherm of the tryptic BSA peptides pretreated by $\text{Fe}_3\text{O}_4@\text{SiO}_2@(\text{dNDS})_n$ particles. The m/z of tryptic BSA peptides are 927.5 (YLVEIAR), 1163.3 (LVNELTEFAK), 1479.6 (LGEYGFQNALIVR) and 1567.7 (DAFLGSFLYEYSR).
168x103mm (96 x 96 DPI)

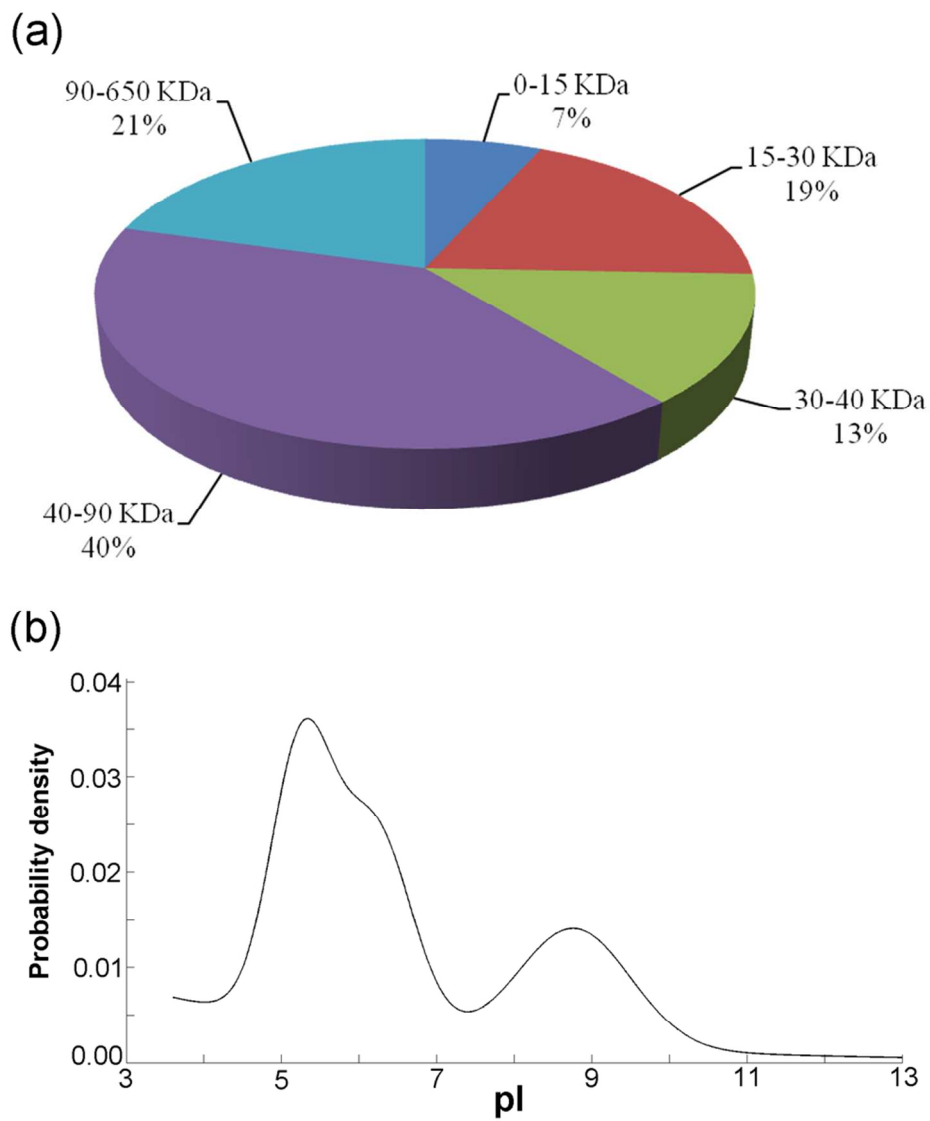


MALDI-TOF mass spectrometry of 2 fmol/ μ L tryptic BSA peptides (1mL) in the presence of saturated NaCl solution (a) without any pretreatment and (b) pretreated by $\text{Fe}_3\text{O}_4@\text{SiO}_2@(\text{dND})_n$ (10 μg). (The asterisks in mass spectra denote peptides which can be identified in database.)
198x246mm (96 x 96 DPI)



SDS-PAGE analysis of the mixture of standard protein (BSA, β -casein and Cyto C). (a) directly analysis of standard protein with a series of mixture protein 0.2S (L1), 0.4S (L2), 0.6S (L3), 0.8S (L4), 1.0S (L5), 2.0S (L6), 4.0S (L7), respectively. The amount of BSA, β -casein and Cyto C in 1S sample is 0.75 μ g, 0.5 μ g and 1.25 μ g, respectively. (b) analysis of the mixture of proteins eluated from Fe₃O₄@SiO₂@(dNDs)_n microsphere pretreated in the 1mL of 4.0S sample sequentially by 20% ACN aqueous solution containing 0.1% TFA and (c) 50% ACN aqueous solution containing 0.1% TFA. To evaluate the recovery and reproducibility of the novel enrichment approach, the process of the method repeated 5 times.

271x304mm (96 x 96 DPI)



Distribution of MW (a) and p I (b) of the secreted proteins in Huh-7 cells pretreated by Fe₃O₄@SiO₂@(dND)_n particles.
90x101mm (300 x 300 DPI)